Parstatin Suppresses Ocular Neovascularization and Inflammation

Hu Huang,[1] Panagiotis Vasilakis,[2] Xiufeng Zhong,[1] Ji-Kui Shen,[1] Katerina Geronatsiou,[3] Helen Papadaki,[3] Michael E. Maragoudakis,[4] Sotirios P. Gartaganis,[2] Stanley A. Vinores,[1] and Nikos E. Tsopanoglou[4]

Purpose. Parstatin is a 41-mer peptide formed by proteolytic cleavage on activation of the PAR1 receptor. The authors recently showed that parstatin is a potent inhibitor of angiogenesis. The purpose of the present study was to evaluate the therapeutic effect of parstatin on ocular neovascularization.

Methods. Choroidal neovascularization was generated in mice using laser-induced rupture of Bruch's membrane and was assessed after 14 days after perfusion of FITC-dextran. Oxygen-induced retinal neovascularization was established in neonatal mice by exposing them to 75% O_2 at postnatal day (P)7 for 5 days and then placing them in room air for 5 days. Evaluation was performed on P17 after staining with anti-mouse PECAM-1. The effect of parstatin was tested after intravitreal administration. The effects of subconjunctival-injected parstatin on corneal neovascularization and inflammation in rats were assessed 7 days after chemical burn-induced corneal neovascularization. Retinal leukostasis in mice was assessed after perfusion with FITC-conjugated concanavalin A.

Results. Parstatin potently inhibited choroidal neovascularization with an IC_{50} of approximately 3 μg and a maximum inhibition of 59% at 10 μg. Parstatin suppressed retinal neovascularization with maximum inhibition of 60% at 3 μg. Ten-microgram and 30-μg doses appeared to be toxic to the neonatal retina. Subconjunctival parstatin inhibited corneal neovascularization, with 200 μg the most effective dose (59% inhibition). In addition, parstatin significantly inhibited corneal inflammation and VEGF-induced retinal leukostasis. In all models tested, scrambled parstatin was without any significant effect.

Conclusions. Parstatin is a potent antiangiogenic agent of ocular neovascularization and may have clinical potential in the treatment of angiogenesis-related ocular disorders. (*Invest Ophthalmol Vis Sci.* 2010;51:5825–5832) DOI:10.1167/iovs.10-5576

Angiogenesis, the formation of new blood vessels, is a well-established and clinically relevant feature of a variety of disease states.[1] For instance, a plethora of studies support the notion that the rate of tumor growth and resultant cancer progression is dependent on the establishment of new blood vessels to supply oxygen and nutrients to proliferating cancer cells.[2] Additionally, aberrant neovascularization, remodeling, fibrosis, and inflammation occur in association with retinal and choroidal ischemic or degenerative diseases such as age-related macular degeneration, diabetic retinopathy, and retinopathy of prematurity[3] and result from infection and mechanical or chemical injury to the cornea.[4]

Proteinase-activated receptor 1 (PAR1) is a G protein–coupled receptor that participates in hemostasis and vascular development[5] and mediates the angiogenic activity of thrombin.[6] PAR1, which is expressed on a variety of cell types including vascular endothelial and smooth muscle cells, is activated through proteolytic cleavage of the Arg41/Ser42 bond on its N-terminal extracellular domain by a variety of proteases, most notably thrombin.[7] The new truncated N terminus serves as a tethered ligand that activates PAR1 itself. However, little is known about the role of the 41-amino acid peptide released during PAR1 activation.

Recently, we have shown that this peptide, for which we coined the name *parstatin*, is a potent antiangiogenic factor.[8] In several in vitro and ex vivo assay systems, including chick embryo chorioallantoic membrane assay, rat aortic ring, and endothelial cell tube formation, parstatin was able to suppress both fibroblast growth factor (FGF)-2– and vascular endothelial growth factor (VEGF)–mediated angiogenesis. Parstatin also suppressed endothelial cell growth by inhibiting the phosphorylation of extracellular signal-regulated kinases (Erk1/2, MAPK) in a specific and reversible fashion and by promoting cell cycle arrest and apoptosis through a mechanism involving the activation of caspases. Based on these findings and the fact that parstatin is an endogenously formed peptide with relative cell-type specificity and high efficacy, we hypothesized that this agent had therapeutic potential in the treatment of neovascular ocular diseases. In the present study, we evaluated the effect of parstatin in well-established models of ocular neovascularization and inflammation.

Materials and Methods

Parstatin Peptides and Animals

The synthesized peptides used were as follows: human parstatin (Biosynthesis Inc., Lewisville, TX), which corresponds to 1–41 amino acids cleaved N-terminal fragment of human PAR1 (sequence, MGPRRLLLVAACFSLCGPLLSARTRARRPESKATNATLDPR); scrambled human parstatin (Peptide Specialty Laboratories GmbH, Heidelberg, Germany), which contains a randomly rearranged amino acid

From the [1]Department of Ophthalmology, Wilmer Eye Institute, Johns Hopkins University School of Medicine, Baltimore, Maryland; and the Departments of [2]Ophthalmology, [3]Anatomy, Histology and Embryology, and [4]Pharmacology, Medical School, University of Patras, Rio-Patras, Greece.

Presented in part at the annual meeting of the Association for Research in Vision and Ophthalmology, Fort Lauderdale, Florida, May 2010.

Supported by University of Patras, Program "K. Karatheodoris" (NET); National Institutes of Health Grants EY017164 and P30EY1765 from the National Eye Institute; and an unrestricted grant from Research to Prevent Blindness (SAV).

Submitted for publication March 24, 2010; revised May 12, 2010; accepted May 14, 2010.

Disclosure: **H. Huang**, None; **P. Vasilakis**, None; **X. Zhong**, None; **J.-K. Shen**, None; **K. Geronatsiou**, None; **H. Papadaki**, None; **M.E. Maragoudakis**, P; **S.P. Gartaganis**, P; **S.A. Vinores**, P; **N.E. Tsopanoglou**, P

Corresponding author: Nikos E. Tsopanoglou, Department of Pharmacology, Medical School, University of Patras, 26500 Rio-Patras, Greece; ntsopan@med.upatras.gr.

sequence to human parstatin (sequence, LRTNASLLVPFLTARAKSSGTREAADPPRLMCLRPLARRCG).

Pathogen-free animals (mice and rats) were housed under conditions of controlled temperature (21°C) in a normal 12-hour light/12-hour dark cycle. All animal studies were conducted in accordance with current guidelines of the ARVO Statement for the Use of Animals in Ophthalmic and Vision Research and the guidelines of the Animal Care and Use Committee at University Medical School.

Mouse Model of Choroidal Neovascularization

Choroidal neovascularization (CNV) was induced by laser photocoagulation-induced rupture of Bruch's membrane.[9,10] C57BL/6J (4- to 5-week-old) mice were anesthetized with ketamine hydrochloride (100 mg/kg body weight) and xylazine (4 mg/kg body weight), and the pupils were dilated with 1% tropicamide. Laser photocoagulation (75-μm spot size, 0.1-second duration, 120 mW) was performed in the 9, 12, and 3 o'clock positions of the posterior pole of the retina with the slit lamp delivery system of a diode laser (Oculight GL; Iridex, Mountain View, CA) and a handheld coverslip as a contact lens to view the retina. Production of a bubble at the time of laser, which indicates the rupture of Bruch's membrane, is an important factor in obtaining CNV. Therefore, only burns in which a bubble was produced were included in the study. Two weeks after the rupture of Bruch's membrane, anesthetized mice were perfused with 50 mg/mL fluorescein-labeled-dextran (2×10^6 average molecular weight, Sigma-Aldrich, St. Louis, MO). The eyes were then dissected and fixed in 10% formalin for 3 hours, and choroidal flatmounts were examined by fluorescence microscopy. Imaging software (Image-Pro Plus; Media Cybernetics, Silver Spring, MD) was used by personnel masked to the study treatments and groups to measure the total area of CNV at each rupture site. Intravitreal injections of 1-μL solutions of parstatin or scrambled parstatin in PBS or PBS alone were administered with a Harvard pump microinjection apparatus. Intravitreal injections were administered immediately after laser treatment and 7 days after laser treatment. CNV was assessed 14 days after laser treatment.

Mouse Model of Oxygen-Induced Retinal Neovascularization

The oxygen-induced ischemic retinopathy model was produced in C57BL/6 mice according to the method described previously.[11] In brief, litters of postnatal day (P)7 mice were exposed to an atmosphere of 75% oxygen in an airtight incubator for 5 days (P12), after which they were returned to room air for 5 days (P17). For quantification of oxygen-induced retinal neovascularization, mice on P17 were given intraocular injection of 1 μL rat anti-mouse platelet endothelial cell adhesion molecule-1 (PECAM-1) antibody (PharMingen, San Jose, CA) under a dissecting microscope with Harvard pump microinjection apparatus. Mice were euthanatized 12 hours after injection and eyes were fixed in PBS-buffered formalin for 5 hours. Retinas were dissected, washed, and incubated with goat anti-rat polyclonal antibody conjugated with AlexaFluor488[12] or were labeled with *Griffonia simplicifolia* 594 (Invitrogen, Carlsbad, CA)[13] for 45 minutes. Both methods gave similar results. Retinal flatmounts were prepared and assessed with fluorescence microscopy and imaging software. Intravitreal injections of 1-μL solutions of parstatin or scrambled parstatin in PBS or PBS alone were administered on P12 (immediately after the mice were removed from hyperoxic conditions) and on P15.

Rat Model of Chemical Burn-Induced Corneal Neovascularization

Pathogen-free male Sprague–Dawley rats (250–300 g) were anesthetized with intramuscular injection of ketamine (25 mg/kg) and xylazine hydrochloride (10 mg/kg). All eyes were examined to exclude any with corneal scars or preexisting neovascularization. Induction of corneal neovascularization was induced with the use of a modification of a previously described procedure.[14] The cornea was cauterized under a microscope by pressing an applicator stick coated with 75% silver nitrate and 25% potassium nitrate to the center of the cornea for 4 seconds. Excess silver nitrate was removed by rinsing the eyes with 5 mL of 0.9% saline. To increase the reproducibility of the injuries, all burns were made by one investigator. The injured eyes then received topical tobramycin 0.3% to prevent infection. Immediately after the burns, rats were randomly divided into groups, and each injured eye was twice subconjunctivally injected with 20-μL solutions of parstatin or scrambled parstatin in PBS or PBS alone. Injections were performed in the 12 and 6 o'clock positions 1 mm posterior to the limbus with a 30-gauge needle attached to a 1-mL tuberculin syringe under a microscope. Seven days later, each eye underwent slit-lamp examination, and photographs of the cornea were taken with a digital camera (D2X; Nikon, Tokyo, Japan) attached to a microscope.

Corneal neovascularization was assessed using a semiautomatic program, which was developed in MATLAB 7.5. The program included conversion of the color image into a black-and-white image, selection of a threshold level that made possible the visualization of the corneal vessels, and calculation of the corneal neovascularization (as a percentage of the number of pixels of the new vessels to the pixels of the total corneal area). The total corneal area was outlined, with the innermost vessel of the limbal arcade used as the border. All calculations were made by a masked observer.

Histopathology

After these processes were performed, the rats were killed and the eyes were excised. All eyes were sectioned (4 μm) and stained with hematoxylin and eosin. Two independent pathologists, in a masked manner, evaluated the microvessel density and the inflammatory cell infiltration in each slide. Total corneal vascular vessels and neutrophils were counted at 200× in seven representative stained tissue sections for each eye, covering the entire corneal area and at a similar distance from the central burn.

Quantitative Measurement of Retinal Leukostasis

C57BL/6J (4- to 5-week-old) mice were anesthetized with ketamine hydrochloride (100 mg/kg body weight) and xylazine (4 mg/kg body weight), and the pupils were dilated with 1% tropicamide. Intravitreal injections of 1-μL solutions of 10 μM VEGF, which is the optimal concentration for promoting leukostasis,[15] or parstatin or scrambled parstatin in PBS or PBS alone, or the combinations, were administered to assess leukostasis. Six hours after intravitreal injections, which was the optimal time determined for VEGF-induced leukostasis, animals were perfused with PBS to remove intravascular content, including nonadherent leukocytes. Perfusion with FITC-conjugated concanavalin A (40 μg/mL in PBS; Vector Laboratories, Burlingame, CA) was then performed to label adherent leukocytes and vascular endothelial cells; this was followed by the removal of residual unbound lectin with PBS perfusion.[15] Retinal flatmounts were prepared and examined under a microscope (Axioskop; Zeiss), and images were digitized. The total numbers of leukocytes adhering to the retinal vessels were counted at 200× by the same investigator, who was masked as to the nature of the specimen.

Statistical Analysis

Data are expressed as mean ± SE, with n numbers as indicated. Statistical analysis was performed using independent samples t-test for parametric data or Kruskal-Wallis and Mann-Whitney U tests for nonparametric data (SPSS 17.0 statistical software; SPSS, Chicago, IL). Differences were considered significant when $P < 0.05$.

Results

Effect of Parstatin on Choroidal Neovascularization

CNV occurs in diseases of Bruch's membrane and of the retinal pigment epithelium, such as age-related macular degeneration. Laser photocoagulation–induced rupture of

Bruch's membrane was used to generate experimental CNV in mice. Intravitreal injections of different doses of parstatin were administered immediately after laser treatment and 7 days after laser treatment. CNV was assessed 14 days after laser treatment. Retinal whole mounts from fluorescein dextran–perfused mice treated with parstatin had areas of NV that were much smaller than those seen in control mice treated with vehicle (PBS) (Figs. 1A–C). Measurements of the area of CNV by image analysis confirmed that there was significantly less neovascularization in eyes treated with parstatin than in control mice (Fig. 1E). The inhibitory effect of parstatin was dose dependent, and the maximum inhibition of CNV was demonstrated with the 10-μg dose, which showed 59% inhibition ($P = 0.015$). The 30-μg dose did not provide additional benefit (Fig. 1E). Mice treated with scrambled parstatin (10 μg) had CNV similar to that obtained in control mice (Figs. 1D, 1E; $P = 0.6$). Slit-lamp examinations showed that all parstatin doses were well tolerated, and no signs of irritation, inflammation, or other ocular toxicity and no signs of systemic toxicity were seen.

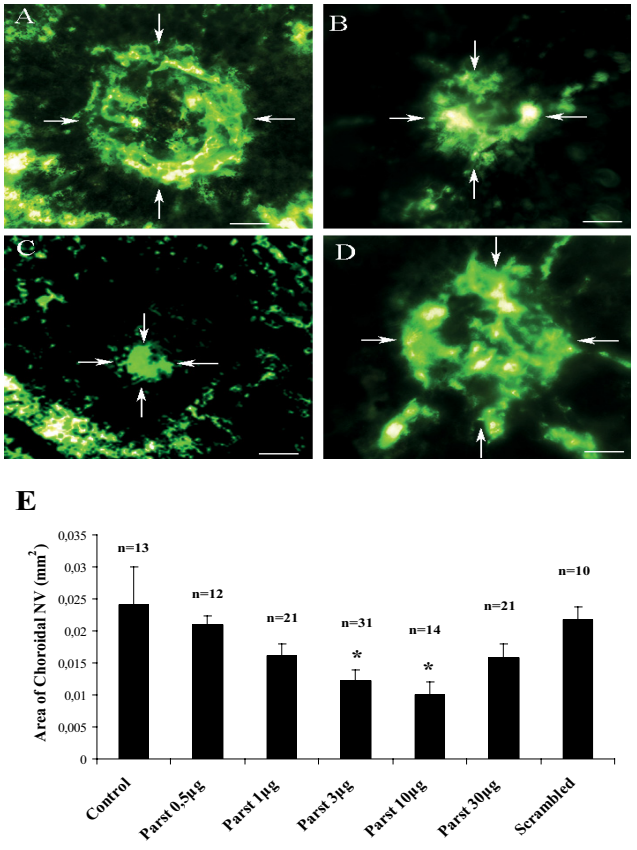

FIGURE 1. Intravitreal injections of parstatin suppress CNV. Laser-induced ruptures of Bruch's membrane were performed in mice. Intravitreal injections of indicated doses of parstatin (parst) or vehicle (control) or scrambled parstatin (scrambled, 10 μg) were administered immediately after laser treatment and 7 days after laser treatment. CNV was assessed 14 days after laser treatment. Mice were perfused with FITC-labeled dextran, and choroidal flatmounts were prepared and examined by fluorescence microscopy. Compared with control eyes (**A**), those injected with 1 μg (**B**) or 10 μg (**C**) parstatin showed proportionally smaller areas of CNV. CNV in eyes injected with scrambled parstatin (**D**) was similar to that in control mice. (**E**) The area of CNV at each rupture site was measured by image analysis. Results are expressed as mean areas (mm^2) of CNV ± SE for each group calculated from the indicated number (n) of eyes. Statistical analysis was performed compared with the control group. *$P < 0.05$.

Effect of Parstatin on Ischemia-Induced Retinal Neovascularization

Oxygen-induced ischemic retinopathy was used to generate retinal neovascularization as a disease model for retinopathy of prematurity and other retinal neovascular diseases, such as diabetic retinopathy. Litters of P7 mice were exposed to an atmosphere of 75% oxygen in an airtight incubator for 5 days (P12), after which they were returned to room air for 5 days (P17). Exposing neonatal mice to hyperoxia prompted regression or delay of retinal vascular development, followed by abnormal angiogenesis after their return to normal oxygen levels. When mice with ischemic retinopathy were given intravitreal injections of PBS at P12 and P15, retinal flatmounts stained for PECAM-1 or *G. simplicifolia* isolectin B4–589, techniques that selectively stain neovascularization on the surface of the retina,[13] showed extensive areas of neovascularization (Figs. 2A, 2E). However, treatment of mice with increasing doses of parstatin at P12 and P15 caused a dose-dependent inhibition of neovascularization on the surface of the retina (Figs. 2B, 2C, 2F, 2G). Measurements of neovascularization by image analysis showed significant reduction in the area of retinal neovascularization in parstatin-treated mice at doses ranging from 0.5 to 5 μg (Fig. 2I). Maximum inhibition was demonstrated with the 3-μg dose, which showed a 60% inhibition ($P = 0.0005$). The 5-μg dose did not provide additional benefit (Fig. 2I). Doses of 10 μg and 30 μg were not well tolerated when administered to newborn mice. Retinal adherence made the retinas virtually impossible to retrieve. There was also adherence of the eyelids and occasional cataract formation with these doses. Mice treated with scrambled parstatin had retinal neovascularization similar to that obtained in control mice treated with PBS (Figs. 2D, 2H, 2I).

Effect of Parstatin on Chemical Burn-Induced Corneal Neovascularization and Inflammation

The time course of corneal neovascularization after cauterization is highly reproducible and well characterized.[16] In the first 24 hours after injury, the limbal vessels that surround the cornea appear slightly engorged. Within 48 hours, the limbal arcades are extended further into the cornea, with many vascular sprouts directing centrally toward the site of injury. By 3 and 4 days after cautery, this dense brushwork of vessels elongates evenly into the cornea from all sides. New blood vessels cover almost 30% of the total cornea area by day 7 (Fig. 3A). The effect of parstatin on corneal neovascularization was evaluated by comparing the total neovascularization area between the parstatin-treated and control (PBS) groups 7 days after corneal cauterization. Results showed that the onset and progression of corneal neovascularization were markedly delayed in the group treated with 2 × 75 μg and 2 × 100 μg parstatin (Figs. 3B, 3C). Measurements of total corneal neovascularization area by image analysis showed a 59% decreased neovascularization area in the parstatin group (2 × 100 μg; $P <$ 0.001) compared with the control group (Fig. 3E). No significant differences were found between the control group and the groups treated with 2 × 50 μg and 2 × 200 μg parstatin (Fig. 3E). Again, rats treated with scrambled parstatin had corneal neovascularization areas similar to those obtained in control rats (Figs. 3D, 3E).

In line with the image analysis data, hematoxylin and eosin staining of corneas revealed that there was more cellularity and thickening in control animals (Figs. 4A, 4D) than in parstatin-treated rats (Figs. 4B, 4E). All corneas in the control group had large numbers of intrastromal blood vessels (Fig. 4A), whereas comparatively less corneal neovascularization infiltration was apparent in the corneal stroma after all parstatin treatment regimens (Fig. 4B). Mean density

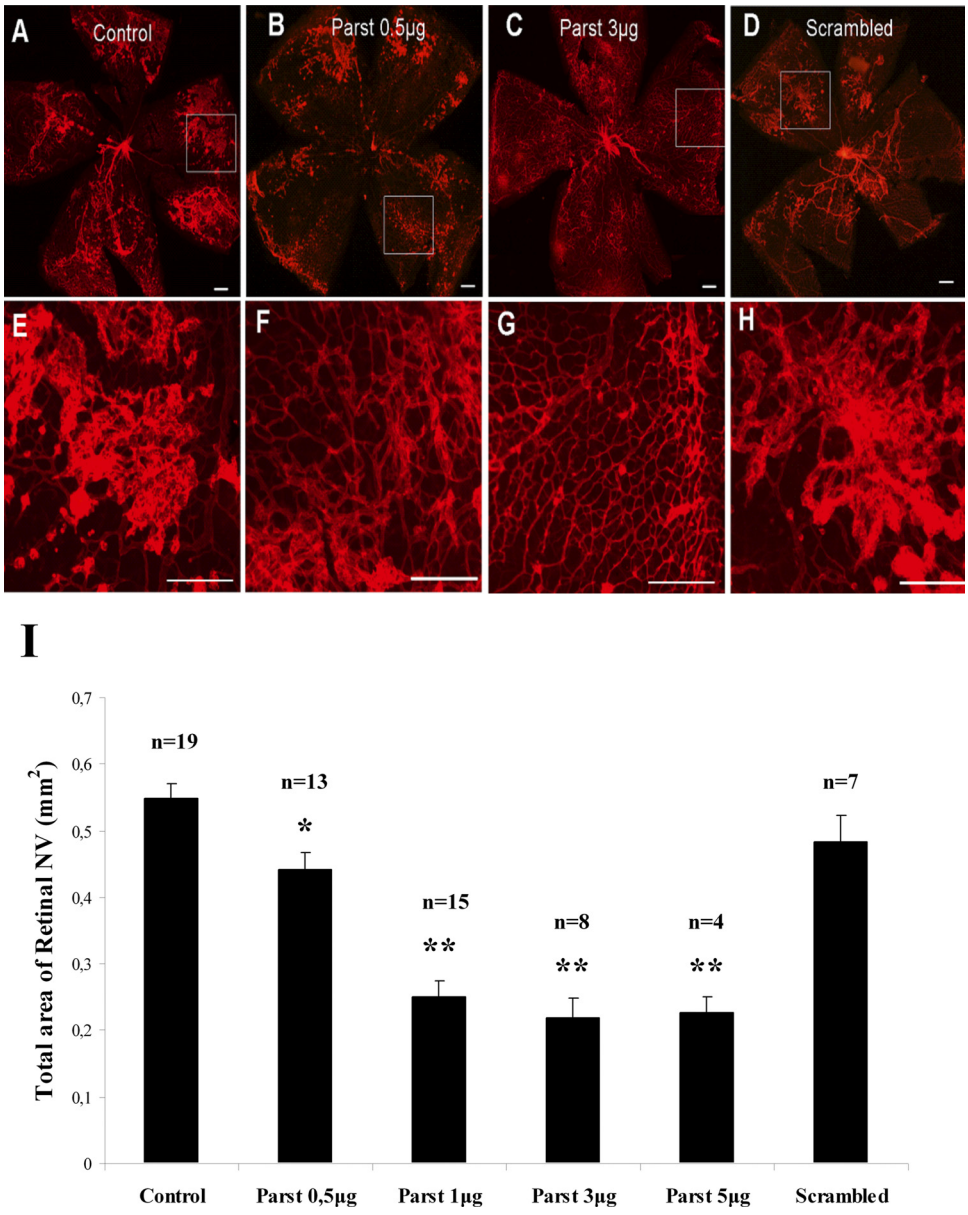

FIGURE 2. Intravitreal injections of parstatin suppress oxygen-induced retinal neovascularization. Newborn mice were placed in 75% oxygen at P7. At P12, they were returned to room air. Intravitreal injections of indicated doses of parstatin (parst), vehicle (control), or scrambled parstatin (scrambled, 10 μg) were administered on P12 and P15. At P17, mice were treated with *G. simplificolia* isolectin B4–589. Compared with control retinas (**A**, **E**), those treated with 0.5 μg (**B**, **F**) or 3 μg (**C**, **G**) parstatin showed proportionally fewer areas of retinal neovascularization. Retinal neovascularization in retinas treated with scrambled parstatin (**D**, **H**) was similar to that observed in control mice. (**E**–**H**) Higher magnification images of the *boxes* in (**A**) to (**D**), respectively. Scale bar, 200 μm. (**I**) Total area of neovascularization (NV) at each retina site was measured by image analysis. Results are expressed as mean areas (mm^2) of retinal neovascularization ± SE for each group calculated from indicated number (*n*) of eyes. Statistical analysis was performed compared with control group. $^*P < 0.05$; $^{**}P < 0.01$.

of vascular vessels (32.14 ± 1.73) was reduced by 56.8% ($P < 0.001$) with parstatin administration (2 × 100 μg) compared with the mean number of vascular vessels (74.3 ± 3.52) in the control sections (Fig. 4G). In scrambled parstatin treatment (2 × 100 μg), 77.17 ± 3.11 was counted as the mean vascular vessel number within the sections, which was not significantly different from that of the control animals (Figs. 4C, 4G). There was no sign of cytotoxicity in any of the treatment groups. Endothelial cells and epithelial layers exhibited no histologic alteration other than some preparation artifacts.

In addition, in this model, an inflammatory response is considered an important prerequisite for neovascularization.[17] One interesting observation in our experiments concerned the superior corneal transparency in the parstatin group compared with the control group. This might suggest an additional inhibitory effect of parstatin on concomitant corneal scarring, possibly related to the inhibition of inflammatory migration and invasion. The beneficial effect of parstatin in this model might relate not only to direct antiangiogenic effects of the peptide but to a potential anti-inflammatory effect. Indeed, the parstatin group (Fig. 4E) had markedly fewer infiltrated inflammatory cell (neutrophils) than did the control (Fig. 4D). The numbers of neutrophils were 6.9 ± 0.57 cells per corneal section in the parstatin-injected corneas (2 × 100 μg) and 36.25 ± 1.32 cells per corneal section in the PBS-injected control corneas (Fig. 4H; $P < 0.001$). In the scrambled parstatin group, the inflammatory cells were 39 ± 2.54 cells per corneal section (Figs. 4F, 4H).

Effect of Parstatin on VEGF-Induced Retinal Leukostasis

Inflammatory leukocyte accumulation is a common feature of major ocular diseases. For instance, leukocytes have been shown to play a role in the pathogenesis of ischemic retinopathies.[18] VEGF, which is a potent chemoattractant for leukocytes, is increased in ischemic retina and is necessary for retinal neovascularization to occur.[19] To investigate the effect of parstatin on leukocyte recruitment, we quantified firm leukocyte adhesion in retinal vessels of VEGF-treated mice using the concanavalin A-staining technique. Six hours after VEGF injec-

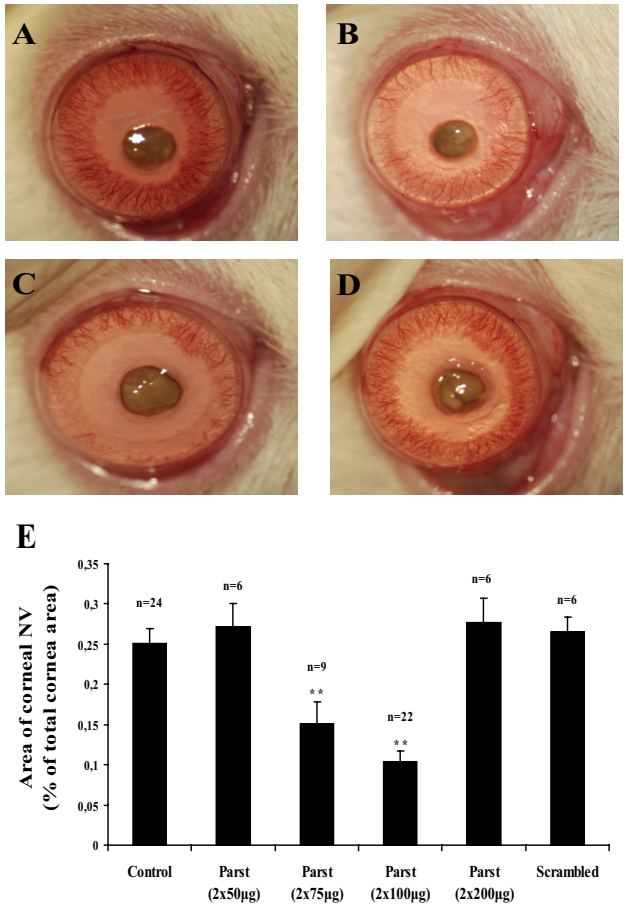

FIGURE 3. Subconjunctival injections of parstatin suppress corneal neovascularization. Chemical burn–induced corneal trauma was performed by the application of 75% silver nitrate and 25% potassium nitrate to the centers of the rat corneas. Two subconjunctival injections per eye of indicated doses of parstatin (parst) or vehicle (control) or scrambled parstatin (scrambled, 2 × 100 μg) were administered immediately after cauterization. Corneal neovascularization was assessed 7 days after cauterization. Compared with control corneas (**A**), those treated with 2 × 75 μg (**B**) or 2 × 100 μg (**C**) parstatin showed proportionally reduced areas of corneal neovascularization. Corneal neovascularization in eyes treated with scrambled parstatin (**D**) was similar to that observed in control mice. (**E**) Total area of neovascularization (NV) in each cornea was measured by image analysis. Results are expressed as the mean percentage of area covered by vessels to the total corneal area ± SE for each group calculated from the indicated number (*n*) of eyes. Statistical analysis was performed compared with the control group. $^{**}P < 0.01$.

tion (10 μM), a large number of leukocytes firmly adhered to the retinal vessels (181 ± 16 cells/retina) compared with vehicle (PBS)-treated controls (5 ± 1 cells/retina) and parstatin alone (8.5 ± 1.6 cells/retina) (Figs. 5A, 5B, 5D). However, when VEGF-treated animals were coinjected with 10 μg parstatin, the number of firmly adhering leukocytes was significantly reduced by 28.7% (129 ± 14 cells/retina; $P = 0.014$) compared with the VEGF-treated controls (Figs. 5C, 5D).

DISCUSSION

Ocular neovascularization, comprising retinal, choroidal, and corneal neovascularization, is associated with enormous public health problems that severely affect the quality of life of the patients.[20] For example, retinal neovascularization is developed in ischemic retinopathies such as diabetic retinopathy and retinopathy of prematurity, which represent the leading causes of severe vision loss and blindness in adults of working age and premature neonates, respectively.[21,22] CNV complicates several diseases, such as age-related macular degeneration, the most common cause of severe loss of vision in patients older than 60 in developed countries.[23] Corneal neovascularization is a serious complication of many corneal diseases as a result of mechanical- or chemical-induced corneal injury and is associated with a high risk factor for graft rejection after corneal allograft transplantation.[24,25]

The present study provides the first strong evidence that parstatin, a synthetic peptide that corresponds to the cleaved peptide on PAR1 activation, has therapeutic potential in the treatment of neovascular ocular diseases. Intraocular injection of parstatin strongly suppressed ischemia-induced retinal neovascularization in neonatal mice. Dose dependency with high potency and efficacy were observed in the ischemic retinopathy model in which maximal inhibition of approximately 60% was achieved with 3 μg parstatin. Similarly, intravitreal or subconjunctival administration of parstatin inhibited CNV at Bruch's membrane rupture sites in mice and potently delayed the onset and progression of neovascularization in rat corneas with chemical burn–induced trauma. The antiangiogenic effects of parstatin in these experimental models of ocular neovascularization are comparable to those of the most effective treatments currently known, such as anti-VEGF, anti-VEGF receptor-2, and anti-PIGF.[26,27] The extent of the inhibition of ocular neovascularization by parstatin attainable in these experiments may be an underestimation of the inhibition expected in primates and in humans. Parstatin peptide used in these experimental rodent models corresponds to the cleaved fragment of human PAR1, which shares 63% and 67% homology to the mouse and rat parstatin, respectively. We have demonstrated that, despite the cross-species activity of parstatin, there is considerable species specificity in vitro.[8] Maximum inhibition of corneal neovascularization was demonstrated using 200 μg parstatin. This dose would be considered high enough compared with doses used in retinal and choroidal neovascularization models. It is possible that periocular (subconjunctival) or intraocular (intravitreal) administration of parstatin may result in differences in parstatin potency; therefore, a higher dose may be needed for the corneal model to achieve regression of neovascularization. Dratviman-Storobinsky et al.[28] reported that different routes of bevacizumab administration in the same animal model of corneal neovascularization resulted in differences in the effectiveness of the drug. In this regard, it should also be noted that the retinal/choroidal neovascularization models were developed in mice whereas the corneal neovascularization model was established in rats, which have a much greater eye size and subsequently a larger volume distribution for the administered parstatin. In addition, our results have shown that the application of parstatin in adult animal eyes was well tolerated and without detectable immunoresponses or toxicity in the cornea or retina. However, in an ischemia-induced retinal neovascularization model in neonatal mice, parstatin exhibited toxicity in the retina at concentrations greater than 10 μg. The different toxicologic profile of parstatin between ocular neovascularization animal models cannot be explained, but it is likely that the immature retina is more sensitive to parstatin than the adult tissues. This may be related to the fact that the neonatal retina is still actively developing, and parstatin may interfere with this development. Alternatively, this apparent toxicity may be related to metabolic or permeability differences in the immature retina. No adverse effects, however, have been observed when parstatin is administered to adult animals. Nevertheless, more experimental studies are needed to evaluate the long-term results and safety of parstatin for the treatment of ocular diseases.

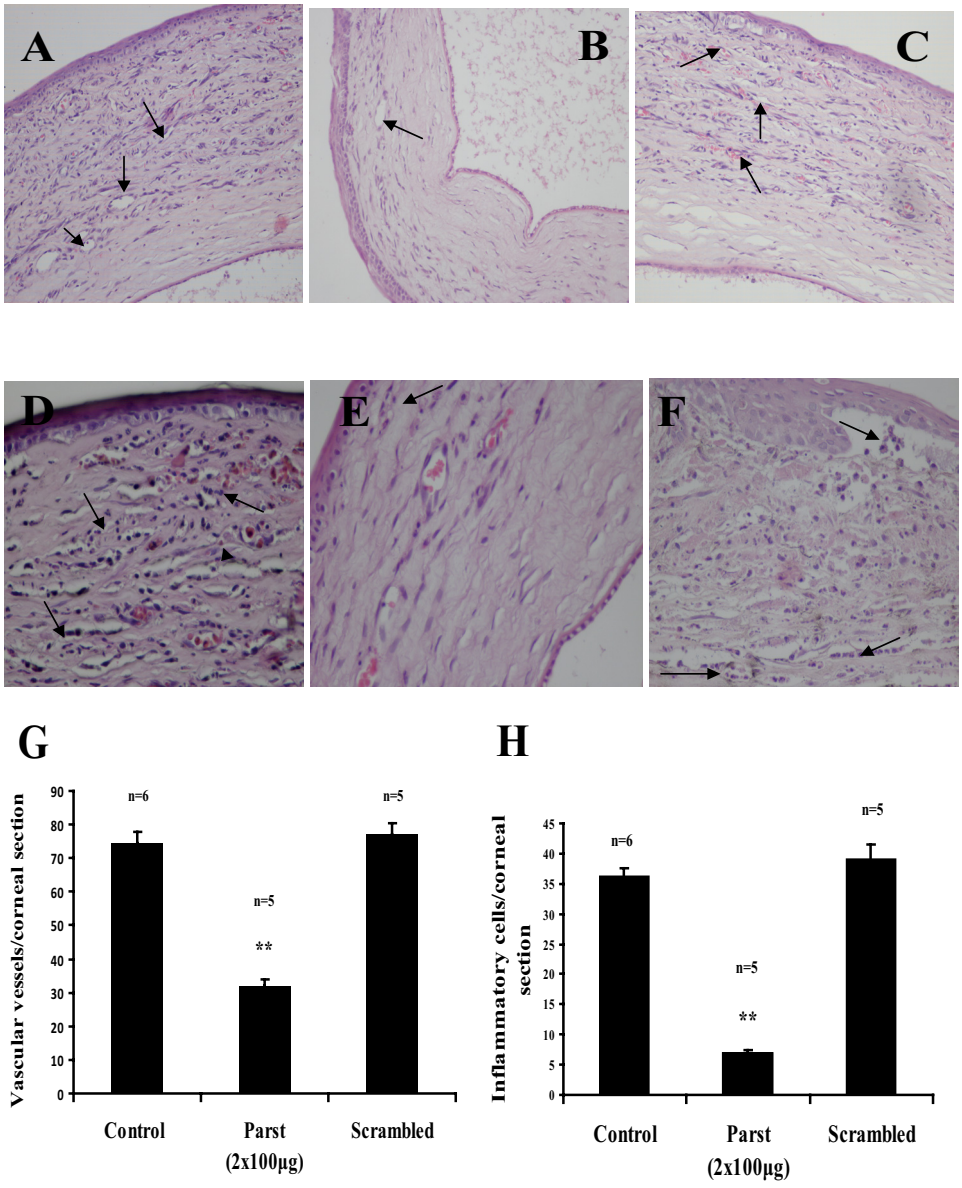

FIGURE 4. Corneal histopathology. Rats were treated as described in Figure 3. Seven days after cauterization, eyes were excised, embedded in paraffin, and sectioned. Sections were stained with hematoxylin-eosin, and vascular vessels (**A**–**C**) or neutrophils (**D**–**F**) in the corneas were counted at 200× or 400× magnification, respectively. Compared with control corneas (**A**, **D**), those treated with 2 × 100 μg (**B**, **E**) parstatin had fewer blood vessels or infiltrating neutrophils. Blood vessel (**C**) or neutrophil (**F**) density in corneas treated with scrambled parstatin were similar to those observed in control rats. (**G**) The total number of blood vessels was measured in seven sections from each eye. Results are expressed as mean number of vascular vessels per section ± SE for each group calculated from indicated number (*n*) of eyes. (**H**) The total number of neutrophils was measured in seven sections from each eye. Results are expressed as mean number of inflammatory cells per section ± SE for each group calculated from indicated number (*n*) of eyes. Statistical analysis was performed compared with the control group. $^{**}P < 0.01$.

We can speculate on the possible mechanisms involved in the inhibitory activity of parstatin on ocular neovascularization. Many factors have been proposed to mediate ocular neovascularization, but VEGF seems to play a critical role since increased VEGF levels have been shown to be a common pathologic factor in neovascular ocular diseases in humans and in animal models, and signaling through VEGF receptors is both necessary and sufficient for the development of aberrant ocular neovascularization.[10,29–31] In line with these observations, the development of potent VEGF antagonists has revolutionized the treatment of CNV caused by age-related macular degeneration[32] and corneal neovascularization caused by various etiologies.[33] However, despite these impressive recent advances, anti-VEGF therapies seem to stabilize the disease process rather than improve vision, indicating that proangiogenic factors other than VEGF may be involved. For example, although the overexpression of FGF2 in the eye does not stimulate neovascularization because it is sequestered,[9,34] FGF2 does contribute to CNV when there is tissue disruption from the disease process itself or attempts at treatment.[35] Parstatin has been demonstrated to have direct effects on endothelial cells.[8] It inhibits survival, proliferation, migration, and tube formation of cultured vascular endothelial cells, and it rapidly localizes to the cell surface, penetrates the cell membrane, and accumulates in the intracellular space. These events may explain the specific interactions between parstatin and signaling mediated by VEGF and FGF2. Pretreatment of endothelial cells with parstatin blocked the activation of Erk1/2 stimulated by either VEGF or FGF2 but had no effect on epidermal growth factor (EGF)- and heparin-binding EGF-driven mitogenic responses. Therefore, combined blockage of VEGF and FGF2 receptor signaling by parstatin may provide greater efficacy for the treatment of ocular neovascularization than does targeting VEGF alone. The precise molecular targets that mediate these cellular effects of parstatin are under investigation. Furthermore, parstatin has been shown to promote cell cycle arrest and apoptosis in endothelial cells through a mechanism involving, at least in part, the activation of caspase-3.[8] However, we have no evidence whether parstatin functions in the same way in animal models of neovascularization. We are planning to perform apoptosis experiments in an oxygen-induced retinal neovascularization model to investigate this issue.

In addition, parstatin is likely to suppress ocular neovascularization through the inhibition of ocular inflammation. Be-

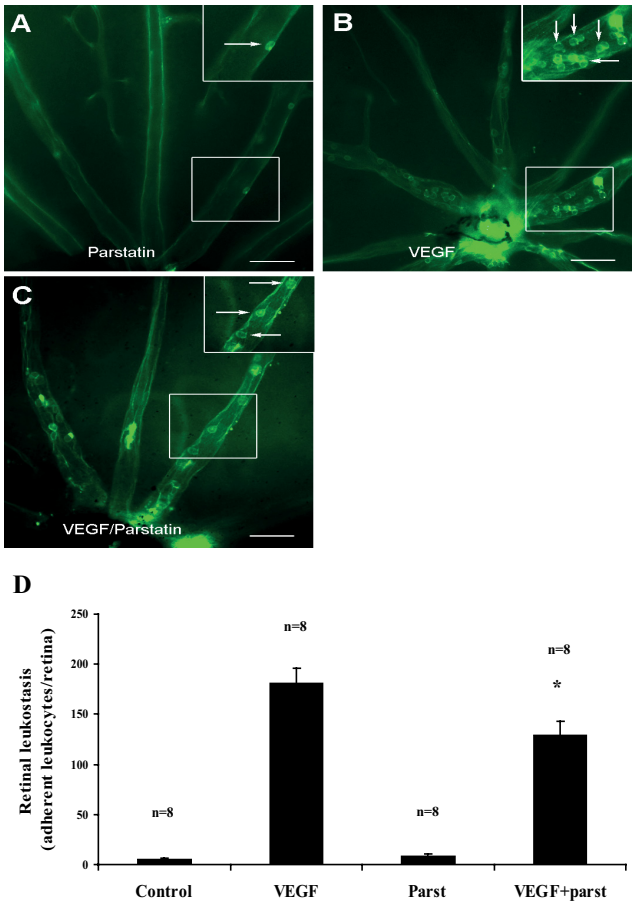

FIGURE 5. Parstatin reduces VEGF-induced retinal leukostasis. Intravitreal injections of vehicle (control), VEGF (10 μM), parstatin (parst, 10 μg), or the combination of VEGF with parstatin were administered to assess their effect on retinal leukostasis. After 6 hours, mice were perfused with FITC-conjugated concanavalin A. Retinal flatmounts were prepared, and the total number of leukocytes adhering to the retinal vessels (*arrows*) was counted at 200× magnification. Few leukocytes adhered to the retinal vessels after injections of vehicle or parstatin (**A**, 200×; *inset*, 400×), whereas pronounced leukostasis was observed after injections of VEGF (**B**, 200×; *inset*, 400×). The combination of parstatin with VEGF resulted in a significant reduction in VEGF-induced leukostasis (**C**, 200×). Scale bar, 200 μm. (**D**) Total numbers of adherent leukocytes were measured in each retina. Results are expressed as mean number of leukocytes per section ± SE for each group calculated from the indicated number (*n*) of eyes. Statistical analysis was performed compared with the control group. $^*P < 0.05$.

cause inflammatory cells play an essential role in the formation of choroidal and retinal neovascularization, the prevention of inflammatory cell recruitment and infiltration into ocular tissues may ameliorate the development of ocular neovascularization.[12,36–38] During inflammation, leukocytes are recruited to the retina in a cascade-like fashion, starting with rolling, followed by firm adhesion and extravasation.[39,40] We have shown in the present study that intraocular injection of parstatin significantly reduced VEGF-induced leukocyte influx into the retina. Furthermore, we found that the application of parstatin markedly reduced the number of inflammatory cells in rat corneas after chemical cauterization. Given that the development of new blood vessels toward the area of the burn is closely associated with increased inflammatory cells within the cornea,[17] our findings suggest that the inhibition of corneal neovascularization by parstatin may be due, at least in part, to the suppression of inflammatory cell recruitment.

In conclusion, in this study we evaluated the pharmacologic efficacy of parstatin for inhibiting ocular neovascularization induced in three well-established animal models. We demonstrated that parstatin effectively suppresses retinal, choroidal, and corneal neovascularization and reduces inflammatory cell recruitment to the ocular lesions. These findings suggest that parstatin may represent a novel attractive and potent therapeutic strategy in the treatment of ocular neovascular and inflammatory diseases.

Acknowledgments

The authors thank Konstantinos Berberides and Dimitris Safaris (Laboratory of Signal processing and Communications, Department of Computer Engineering and Informatics, University of Patras, Greece) for the development of software for imaging corneal neovascularization and Nikolia Sotiropoulou for skillful technical assistance in the preparation of corneal histologic sections.

References

1. Ferrara N, Kerbel RS. Angiogenesis as a therapeutic target. *Nature.* 2005;438:967–974.
2. Folkman J. Angiogenesis. *Ann Rev Med.* 2006;57:1–18.
3. Tolentino MJ. Current molecular understanding and future treatment strategies for pathologic ocular neovascularization. *Curr Mol Med.* 2009;9:973–981.
4. Azar DT. Corneal angiogenic privilege: angiogenic and antiangiogenic factors in corneal avascularity, vasculogenesis, and wound healing (an American Ophthalmological Society thesis). *Trans Am Ophthalmol Soc.* 2006;104: 264–302.
5. Coughlin SR. Protease-activated receptors in hemostasis, thrombosis, and vascular biology. *J Thromb Haemost.* 2005;3:1800–1814.
6. Tsopanoglou NE, Maragoudakis ME. Inhibition of angiogenesis by small-molecule antagonists of protease-activated receptor-1. *Semin Thromb Hemost.* 2007;33:680–687.
7. Vu TK, Hung DT, Wheaton VI, Coughlin SR. Molecular cloning of a functional thrombin receptor reveals a novel proteolytic mechanism of receptor action. *Cell.* 1991;64:841–848.
8. Zania P, Gourni D, Aplin AC, et al. Parstatin, the cleaved peptide on proteinase-activated receptor 1 activation, is a potent inhibitor of angiogenesis. *J Pharmacol Exp Ther.* 2009;328:378–389.
9. Tobe T, Ortega S, Luna JD, et al. Targeted disruption of the FGF2 gene does not prevent choroidal neovascularization in a murine model. *Am J Pathol.* 1998;153:1641–1646.
10. Kwak N, Okamoto N, Wood JM, Campochiaro PA. VEGF is an important stimulator in a model of choroidal neovascularization. *Invest Ophthalmol Vis Sci.* 2000;41:3158–3164.
11. Smith LEH, Wesolowski E, McLellan A, et al. Oxygen-induced retinopathy in the mouse. *Invest Ophthalmol Vis Sci.* 1994;35: 101–111.
12. Shen J, Xie B, Dong A, et al. In vivo immunostaining demonstrates macrophages associate with growing and regressing vessels. *Invest Ophthalmol Vis Sci.* 2007;48:4335–4341.
13. Connor KM, Krah NM, Dennison RJ, et al. Quantification of oxygen-induced retinopathy in the mouse: a model of vessel loss, vessel regrowth and pathological angiogenesis. *Nat Protoc.* 2009; 4:1565–1573.
14. Mahoney JM, Waterbury LD. Drug effects on the neovascularization response to silver nitrate cauterization of the rat cornea. *Curr Eye Res.* 1985;4:531–535.
15. Vinores SA, Xiao W-H, Shen J, Campochiaro PA. TNFα is critical for ischemia-induced leukostasis, but not retinal neovascularization nor VEGF-induced leakage. *J Neuroimmunol.* 2007;182:73–79.
16. Ross LL, Danehower SC, Proia AD, et al. Coordinated activation of corneal wound response genes in vivo as observed by in situ hybridization. *Exp Eye Res.* 1995;61:435–450.
17. Murthy RC, McFarland TJ, Yoken J, et al. Corneal transduction to inhibit angiogenesis and graft failure. *Invest Ophthalmol Vis Sci.* 2003;44:1837–1842.
18. Majka S, McGuire PG, Das A. Regulation of matrix metalloproteinase expression by tumor necrosis factor in a murine model of

retinal neovascularization. *Invest Ophthalmol Vis Sci.* 2002;43: 260–266.

19. Joussen AM, Murata T, Tsujikawa A, et al. Leukocyte-mediated endothelial cell injury and death in the diabetic retina. *Am J Pathol.* 2001;158:147–152.
20. Zhang SX, Ma JX. Ocular neovascularization: implication of endogenous angiogenic inhibitors and potential therapy. *Prog Retin Eye Res.* 2007;26:1–37.
21. Williams R, Airey M, Baxter H, et al. Epidemiology of diabetic retinopathy and macular oedema: a systemic review. *Eye.* 2004; 18:963–983.
22. Drack A. Retinopathy of prematurity. *Adv Pediatr.* 2006;53:211–226.
23. Gragoudas ES, Adamis AP, Cunningham ET Jr, Feinsod M, Guyer DR. Pegaptanib for neovascular age-related macular degeneration. *N Engl J Med.* 2004;351:2805–2816.
24. Lee P, Wang CC, Adamis AP. Ocular neovascularization: an epidemiologic review. *Surv Ophthalmol.* 1998;43:245–269.
25. Cursiefen C, Cao J, Chen L, et al. Inhibition of hemangiogenesis and lymphangiogenesis after normal-risk transplantation by neutralizing VEGF promotes graft survival. *Invest Ophthalmol Vis Sci.* 2004;45:2666–2673.
26. Vinores SA. Anti-VEGF therapy for ocular vascular diseases. In: Maragoudakis M, Papadimitriou E, eds. *Angiogenesis: Basic Science and Clinical Applications*. Kerala, India: Transworld Research Network; 2007;28:467–482.
27. Van de Veire S, Stalmans I, Heindryckx F, et al. Further pharmacological and genetic evidence for the efficacy of PIGF inhibition in cancer and ocular neovascularization. *Cell.* 2010;141:178–190.
28. Dratviman-Storobinsky O, Lubin BC, Hasanreisoglu M, Goldenberg-Cohen N. Effect of subconjunctival and intraocular bevacizumab injection on angiogenic gene expression levels in a mouse model of corneal neovascularization. *Mol Vis.* 2009;15:2326–2338.
29. Aiello LP. Vascular endothelial growth factor. *Invest Ophthalmol Vis Sci.* 1997;38:1647–1652.
30. Amano S, Rohan R, Kuroki M, Tolentino M, Adamis AP. Requirement for vascular endothelial growth factor in wound- and inflammation-related corneal neovascularization. *Invest Ophthalmol Vis Sci.* 1998;39:18–22.
31. Ozaki H, Seo M-S, Ozaki K, et al. Blockade of vascular endothelial cell growth factor receptor signalling is sufficient to completely prevent retinal neovascularization. *Am J Pathol.* 2000;156:679–707.
32. Rosenfeld PJ, Brown DM, Heier JS, et al. Ranibizumab for neovascular age-related macular degeneration. *N Engl J Med.* 2006;355: 1419–1431.
33. Kim SW, Ha BJ, Kim EK, et al. The effect of topical bevacizumab on corneal neovascularization. *Ophthalmology.* 2006;113:1–12.
34. Ozaki H, Okamoto N, Ortega S, et al. Basic fibroblast growth factor is neither necessary nor sufficient for the development of retinal Neovascularization. *Am J Pathol.* 1998;153:757–765.
35. Yamada H, Yamada E, Kwak N, et al. Cell injury unmasks a latent proangiogenic phenotype in mice with increased expression of FGF2 in the retina. *J Cell Physiol.* 2000;185:135–142.
36. Donoso LA, Kim D, Frost A, Callahan A, Hageman G. The role of inflammation in the pathogenesis of age-related macular degeneration. *Surv Ophthalmol.* 2006;51:137–152.
37. Lima e Silva R, Shen J, Hackett SF, et al. The SDF-1/CXCR4 ligand/receptor pair is an important contributor to several types of ocular neovascularization. *FASEB J.* 2007;21:3219–3230.
38. Noda K, Miyahara S, Nakazawa T, et al. Vascular adhesion protein-1 blockage suppresses choroidal neovascularization. *FASEB J.* 2008; 22:2928–2935.
39. Butcher EC. Leukocyte-endothelial cell recognition: three (or more) steps to specificity and diversity. *Cell.* 1991;67:1033–1036.
40. Springer TA. Traffic signals for lymphocyte recirculation and leukocyte emigration: the multistep paradigm. *Cell.* 1994;76:301–314.